A microwave metamaterial with integrated power harvesting functionality

Allen M. Hawkes,[a] Alexander R. Katko, and Steven A. Cummer
Department of Electrical and Computer Engineering, Duke University, 101 Science Drive, Durham, North Carolina 27708-9976, USA

(Received 30 May 2013; accepted 22 September 2013; published online 14 October 2013)

We present the design and experimental implementation of a power harvesting metamaterial. A maximum of 36.8% of the incident power from a 900 MHz signal is experimentally rectified by an array of metamaterial unit cells. We demonstrate that the maximum harvested power occurs for a resistive load close to 70 Ω in both simulation and experiment. The power harvesting metamaterial is an example of a functional metamaterial that may be suitable for a wide variety of applications that require power delivery to any active components integrated into the metamaterial. © *2013 AIP Publishing LLC*. [http://dx.doi.org/10.1063/1.4824473]

Metamaterials are composed of sub-wavelength particles that exhibit bulk properties that are different from their individual components. Electromagnetic metamaterials are engineered materials that can achieve parameters not possible within naturally occurring materials, such as a negative index of refraction[1] or a zero index of refraction.[2] Exotic properties like these allow for a variety of interesting applications including a superlens device[3] and an invisibility cloak.[4] Integrating active and nonlinear functionality into metamaterials has been demonstrated in the form of dynamic resonant frequency tuning,[5,6] phase conjugation,[7] and wave mixing.[8,9] More specific functional behavior has also been demonstrated in metamaterials, including radio frequency (RF) limiting[10] and harmonic generation.[11]

Metamaterials are also well-suited for other functional behaviors, including electromagnetic power harvesting, the focus of this work. Power harvesting devices convert one type of energy to another, typically converting to a direct current (DC) signal. Many types of energy can be harvested, from acoustic (using a piezoelectric harvester)[12] to electromagnetic (using a rectenna).[13] Power harvesting devices require a method to couple to the energy that will be harvested as well as a device to convert the energy from one form to another. By their very nature, metamaterials are designed to couple to various types of energy, e.g., from acoustic[14] to optical,[15] and thus provide a natural platform for power harvesting. Electromagnetic metamaterials provide flexibility in design due to their electrically small, low-profile nature.[16] Since metamaterials are typically designed as infinite arrays, the resonant frequency and input impedance include coupling effects. Metamaterials can be adapted to various applications, such as flexible sheets to cover surfaces.[17] Moreover, many metamaterials that have been presented in the literature require some form of external signal. This could be a DC bias voltage[18] or a large external pump signal.[7] In general, metamaterials could be modified to harvest such an external signal that is already present for other purposes. With these design advantages, power harvesting metamaterials offer design flexibility for a large number of applications that general antenna-based microwave power harvesting devices may lack.

A recent simulation-based study[19] investigated the conversion efficiency between incident RF power and induced power in a split-ring resonator (SRR). Our work is focused on the experimental measurement of RF to DC efficiency based on the conventional effective area of the SRR. We demonstrate that metamaterials can also include embedded devices to convert the incident RF energy to a DC voltage, providing a platform for power harvesting that utilizes the advantages of metamaterial design.

An SRR is a canonical example of a resonant metamaterial particle and is used as the basis for the unit cells of the metamaterial power harvester designed here. By tuning the SRR parameters, we design an SRR (Fig. 1) to resonate at 900 MHz using an S-parameter simulation within Computer Simulation Technology (CST) Microwave Studio software. Using CST Microwave Studio, we can also simulate the effects of embedding devices within the SRR by retrieving its S-parameters using a lumped port. The retrieved S-parameters are loaded into Agilent Advanced Design System (ADS), allowing us to simulate both fullwave 3D effects and circuit-level nonlinear effects.

An SRR couples strongly to an incident magnetic field and can be loaded with a wide variety of circuit elements. In this work, we embed a rectifying circuit within an SRR to convert the incident RF power to DC power. A number of rectifying circuits could be chosen depending on the particular application for the power harvesting metamaterial. We choose to use a Greinacher[20] circuit because the output voltage is double the input voltage maximum, which allows for

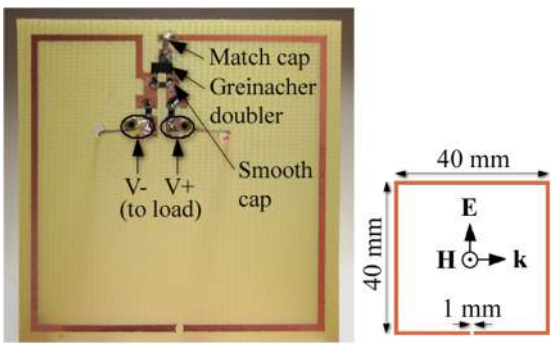

FIG. 1. (Left) Power harvesting SRR. (Right) Plain SRR with dimensions shown, 1 mm traces. Incident wave polarization is also shown.

[a]allen.hawkes@duke.edu

easier power transmission and measurement. A Greinacher circuit has a lower effective capacitance in comparison to other rectification circuits (such as a bridge rectifier), allowing faster switching and thus a higher frequency of operation. A Greinacher circuit also has a low threshold voltage, allowing operation at lower incident power levels. A Greinacher voltage doubler can be placed across a gap (Fig. 1) in the top side of the copper trace to rectify the induced current present in the SRR. Schottky diodes are used for the voltage doubler due to their typically low open junction capacitance and fast switching capabilities, which allow for rectification of a high-frequency RF signal, as well as their typically low threshold voltage. A resistive load placed across the output of the voltage doubler is a simple way to determine DC power out using $P = V^2/R$. This DC power is maximized through ADS for matching capacitor and resistor values. The parameters of our selected Schottky diode (HSMS 2862) and the simulated S-parameters of the above SRR in a model of our actual parallel-plate waveguide are input into ADS for the simulation, shown in a schematic in Fig. 2.

The simulated components lead to a maximum efficiency of 61% for an input power of 24.25 dBM, the maximum available experimental power (at an incident power density of approximately 1.6 mW/cm^2). One important figure of merit for a power harvester is its RF-to-DC power conversion efficiency:

$$\eta = \frac{P_{DC}}{P_{RF}}.$$

We determine P_{RF} by measuring the total incident power in our measurement apparatus. For a large metamaterial sample, we assume that the total incident power to the measurement apparatus is incident on the metamaterial. For a single unit cell, it is necessary to use the effective area of the unit cell to determine the incident P_{RF}. The maximum effective area may be calculated by[21]

$$A_{e,max} = \frac{\lambda^2}{4\pi} D_0,$$

where $D_0 = 1.5$ since the SRR is effectively a small loop illuminated by a transverse electromagnetic (TEM) wave. For an SRR resonant at 900 MHz, the effective area is thus $A_{e,max} = 5.3A_{physical}$. The full waveguide area is approximately $6.8A_{physical}$ where $A_{physical}$ is the physical area of a single SRR unit cell. As $A_{e,max}$ is 78% of the open wave guide area, 78% of the incident power density is used as input power for simulation of the single cell.

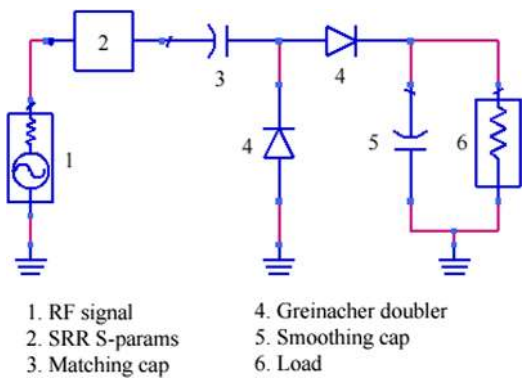

FIG. 2. ADS simulation schematic of SRR power harvester. CST Microwave Studio was used to determine the SRR S-parameters.

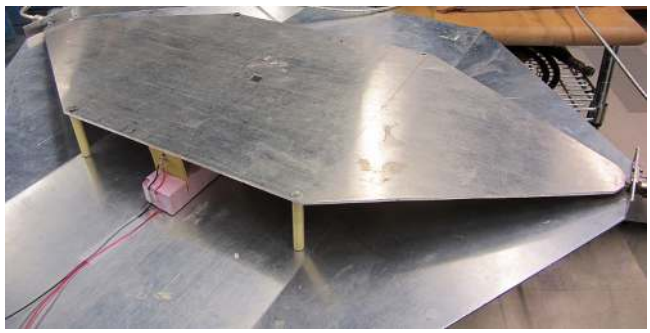

FIG. 3. Placement of SRR within open waveguide.

The designed voltage doubler and resistive load are added to an SRR as shown in Fig. 1, resulting in the power harvesting metamaterial unit cell. To observe power harvesting capabilities, the cell is placed in an open, TEM waveguide (Fig. 3) where input power is produced by a signal generator and amplifier, and output power is measured with an oscilloscope via leads placed across the resistive load (Fig. 4). The DC power harvested is determined by $P = V^2/R$ as previously mentioned, and input power is measured with a spectrum analyzer connected to the signal generator and amplifier via the open waveguide. By increasing the incident power from 13 to 24 dBm and measuring the DC output from the SRR, the normalized harvested power, $P_{DC}/P_{RF,incident}$, as a function of incident power $P_{RF,incident}$ and resulting efficiency are determined at each point. The maximum efficiency of the single cell is 14.2%, setting $P_{RF,incident}$ as 78% of the total input power from effective area calculations.

Multiple power harvesting SRR cells are then tested simultaneously to create the power harvesting metamaterial, which is accomplished through a 5×1 array shown in Fig. 5. Through a parallel connection of the leads from each SRR's resistive load, the total power harvested by the metamaterial is found in the same way as the single cell. The maximum efficiency for the 5×1 array is 36.8%, where P_{in} is the entire input power because the array spans the entire length. Measured efficiencies of both the single and the array of power harvesting SRRs are shown in Fig. 6. Also shown in Fig. 6 is the open circuit voltage, V_{OC}, a load-independent measure of the available voltage harvested by the array of SRRs.

The power harvesting metamaterial array is more efficient than the single unit cell. This is partially due to the

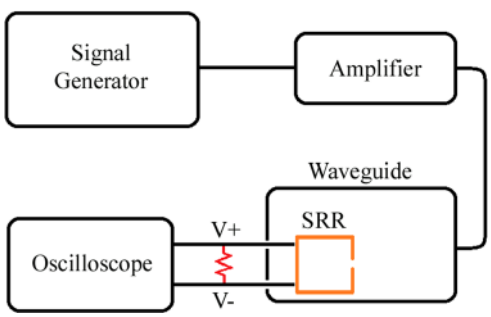

FIG. 4. Experimental test setup schematic.

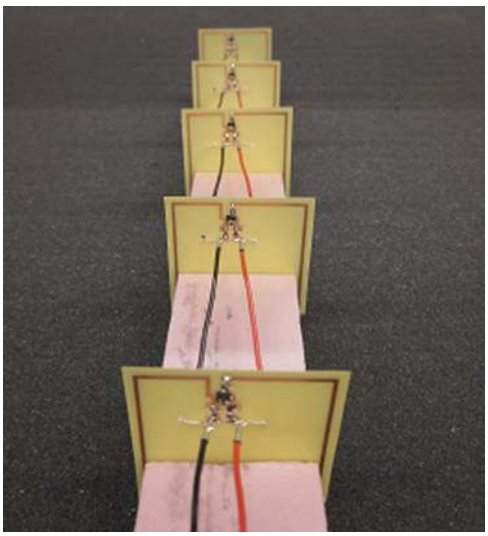

FIG. 5. 5×1 array of power-harvesting SRRs.

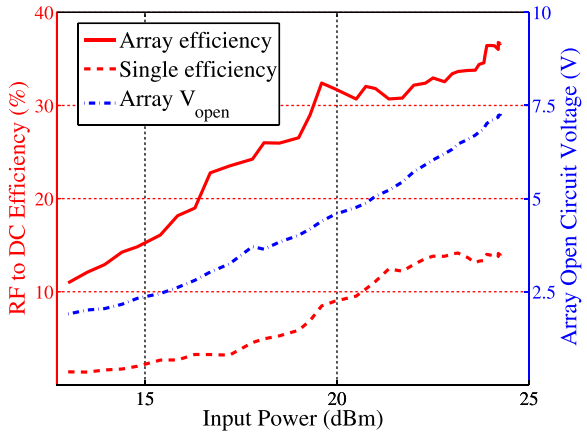

FIG. 6. RF to DC efficiency of power harvesters. The open-circuit voltage of the array is also shown.

larger effective area of the array. While the effective area of the single cell is 78% the entire width of the waveguide, some of this power is not harvested by the single unit cell due to fringing effects on the sides of the waveguide. For this reason, placement of multiple cells that together span the entire waveguide width results in a higher efficiency as the array captures more of the electromagnetic energy that undergoes the fringing effect.

Another important relationship is the efficiency of the power harvesting metamaterial as a function of load resistance. Simulated and experimental efficiencies for the 5×1 array are shown in Fig. 7. Though the experimental efficiencies do not match the values from simulation, the simulation does accurately predict the maximum harvested power as falling approximately within the range of 70–80 Ω, confirmed by the experimental data. The experimental efficiency maximum occurs at 70 Ω, and the simulated maximum occurs at 82 Ω, showing close correspondence.

In summary, we have designed, simulated, and experimentally measured a functional metamaterial power harvester capable of converting up to 36.8% of the incident RF power to DC power. Through a parallel connection of five SRRs, a V_{OC} of 7.3 V is achieved. Simulations match

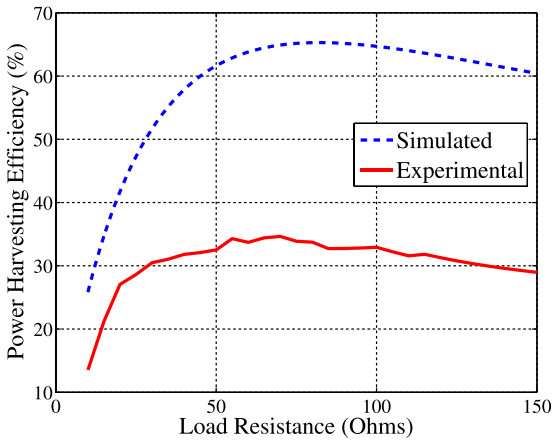

FIG. 7. RF to DC efficiency of SRR array as a function of load resistance, for both simulation and experiment. Note that both show maximum efficiency for around 70–80 Ω.

experimental results showing an optimal resistive load for DC power transfer of 70–80 Ω. The SRR power harvester is an example of functional metamaterial that may be suitable for a wide variety of RF applications that require power delivery to any active integrated components.

This work was supported by a Multidisciplinary University Research Initiative from the Army Research Office (Contract No. W911NF-09-1-0539).

[1]D. R. Smith, W. J. Padilla, D. C. Vier, S. C. Nemat-Nasser, and S. Schultz, Phys. Rev. Lett. **84**, 4184–4187 (2000).
[2]R. W. Ziolkowski, Phys. Rev. E **70**, 046608 (2004).
[3]N. Fang, H. Lee, C. Sun, and X. Zhang, Science **308**(5721), 534–537 (2005).
[4]D. Schurig, J. J. Mock, B. J. Justice, S. A. Cummer, J. B. Pendry, A. F. Starr, and D. R. Smith, Science **314**(5801), 977–980 (2006).
[5]I. V. Shadrivov, S. K. Morrison, and Y. S. Kivshar, Opt. Express **14**(20), 9344–9349 (2006).
[6]H.-T. Chen, J. F. O'Hara, A. K. Azad, A. J. Taylor, R. D. Averitt, D. B. Shrekenhamer, and W. J. Padilla. Nature Photon. **2**(5), 295–298 (2008).
[7]A. R. Katko, S. Gu, J. P. Barrett, B.-I. Popa, G. Shvets, and S. A. Cummer, Phys. Rev. Lett. **105**, 123905 (2010).
[8]D. Huang, A. Rose, E. Poutrina, S. Larouche, and D. R. Smith, Appl. Phys. Lett. **98**(20), 204102 (2011).
[9]A. Rose, D. Huang, and D. R. Smith, Phys. Rev. Lett. **110**, 063901 (2013).
[10]A. R. Katko, A. M. Hawkes, J. P. Barrett, and S. A. Cummer, IEEE Antennas Wireless Propag. Lett. **10**, 1571–1574 (2011).
[11]I. V. Shadrivov, A. B. Kozyrev, D. W. van der Weide, and Y. S. Kivshar, Appl. Phys. Lett. **93**(16), 161903 (2008).
[12]M. Lallart, D. Guyomar, C. Richard, and L. Petit, J. Acoust. Soc. Am. **128**, 2739–2748 (2010).
[13]N. Zhu, R. W. Ziolkowski, and H. Xin, Appl. Phys. Lett. **99**(11), 114101 (2011).
[14]J. Li and C. T. Chan, Phys. Rev. E **70**(5), 055602 (2004).
[15]H. J. Lezec, J. A. Dionne, and H. A. Atwater, Science **316**(5823), 430–432 (2007).
[16]R. W. Ziolkowski and A. Erentok, IEEE Trans. Antennas Propag. **54**(7), 2113–2130 (2006).
[17]G. X. Li, S. M. Chen, W. H. Wong, E. Y. B. Pun, and K. W. Cheah, Opt. Express **20**(1), 397–402 (2012).
[18]J. Zhao, Q. Cheng, J. Chen, M. Q. Qi, W. X. Jiang, and T. J. Cui, New J. Phys. **15**, 043049 (2013).
[19]O. M. Ramahi, T. S. Almoneef, M. Alshareef, and M. S. Boybay, Appl. Phys. Lett. **101**, 173903 (2012).
[20]A. S. Sedra and K. C. Smith, *Microelectronic Circuits*, 6th edition (Oxford University Press, 2009).
[21]C. A. Balanis, *Antenna Theory: Analysis and Design* (Wiley-Interscience, New York, 2005).